Mixing in Micro-scaled Coiled Flow Inverter of Varying Tube Diameter

Joanne Z. E. Soh, Eko Supriyanto

***Abstract*—** Coiled Flow Inverter (CFI) is a tubing configuration which facilitates process intensification. In microfluidics domain, the laminar flow due to low Reynolds number (Re) might inhibit effective mixing in Micro-scaled Coiled Flow Inverter (MCFI). Simulation with Computational Fluid Dynamics (CFD) software FLUENT was implemented to investigate the mixing with MCFI with different diameters. Fluid flow of the mixing of two water bodies was simulated. Geometry of the MCFI was designed with tubing diameters of 1.0mm, 0.8mm, and 0.5mm and a fixed curvature ratio (λ) of 10. Fluid flow rate was adjusted to achieve Re of 250 for each tubing size. Simulation results showed skewed velocity profile MCFI, which facilitated secondary flow and flow inversion. MCFI with the tubing diameter of 0.5 mm achieved complete mixing, at 0.69 normalized tube length equivalent to 175mm. MCFI with ID 1.0 mm showed 54.5% mixing, while MCFI with ID 0.8 mm showed 69.6% mixing. Results suggested smaller tubing diameter led to better mixing process in MCFI.

***Keywords*—** Micro-Coiled Flow Inverter (mCFI), Reynolds number, Dean vortices, and Computational Fluid Dynamics (CFD)

I. Introduction

Mixing within a microfluidic domain generally depends on molecular diffusion to achieve a uniform spatial distribution in solute concentrations. Fluid flow in domain with low Reynolds number results in laminar flow, in which fluid flows in parallel layers without turbulence. Coiled configuration, namely helical mixing element, introduced secondary flow within a laminar flow domain by enforcing a centrifugal force acting outwards to the outer wall of a curvature. However, there exists a region in which fluid mixing progress slowly regardless of prolongation of tubing length, due to the presence of a laminar region which diminished the effect of centrifugal force [1]. Coiled Flow Inverter, as an extension of the helical mixing element, is constructed based on the principle of complete flow inversion. Constructed with coiled tube geometry with 90 degree bends at equal intervals of length, CFI was designed to induce Dean Vortices rotating corresponding to the 90 bending [4].

Studies had proven that the CFI configuration improved mixing [2] and thermal distribution [3], through numerical and experimental methods. In the process industry, computer simulations proved CFI to be beneficial in liquid-liquid mixing. An evaluation of cross-sectional velocity profile and scalar concentration of liquid flow concluded significant increment in mixing as compared to a straight tube and helical mixing element of equal tube length [5]. Experimental works confirmed the enhanced mixing of CFI in which fluids achieve a narrow residence time distribution even under laminar flow [9]. Furthermore, CFI has found application as a reactor for production of biodiesel by the transesterification of fatty acids [10].

CFI has recently been scaled down to micro-dimensions for process intensification [6], specifically as a micro heat exchanger. Micro-coiled flow inverter (MCFI) is constructed from tubing with diameter of equal or less than 1 mm. Results showed that MCFI possessed higher thermal merit. Characterization of residence time distribution curve from different MCFI reactor setup also found that the shape of the reactor had negligible effect on the axial dispersion [7]. MCFI has been applied in a liquid-liquid extraction system, used in addition to the generation of slug flow [8].

In the present work, a computational fluid dynamics (CFD) study was performed in tubing with circular cross-section of different tube diameter constructed into a MCFI to understand the effect of tube diameter towards the mixing of two miscible fluids under laminar flow with similar Re has been reported.

II. Materials and Methods

A. Software

CFD simulation was carried out with the software FLUENT in ANSYS 15. In this study, a liquid-liquid flow system of water-based dyes, here on considered 'red dye' and 'blue dye', was injected into the MCFI, and left to interact. The fluid properties of the water soluble dyes were assumed insignificant due to dilution. Thus, the simulation was carried out with the properties of liquid water including density and dynamic viscosity.

B. Governing Equations

To solve the conservation equations for chemical species,

This research was supported by the Malaysian Ministry of Higher Education under the Research University Grant Vot. No. Q.J130000.2509.10H87.

J. Z. E. Soh is with the Faculty of Biosciences and Medical Engineering, Universiti Teknologi Malaysia, 81310 Johor Bahru Malaysia.(e-mail: joanne.sohze@gmail.com)

Eko Supriyanto is with the Advanced Diagnostics and Progressive Human Care Research Group, IJN-UTM Cardiovascular Engineering Centre, Faculty of Biosciences and Medical Engineering, Universiti Teknologi Malaysia, 81310, Johor Bahru Malaysia (phone: +6016 776 3004, e-mail: eko@utm.my)

species transport model was used for simulation purposes. This model predicts the local mass fraction of each species by solving the convection-diffusion equation for the *i*th species, which is as follows.

Conservation equation:

$$\frac{\partial}{\partial t}(\rho Y_i) + \nabla \cdot (\rho \vec{v} Y_i) = -\nabla \cdot \vec{J}_i + R_i + S_i \tag{1}$$

where the letters ρ ,Y, $\vec{v}$, $\vec{J}$, R and S indicates the density, local species mass fraction, velocity vector, species diffusion flux, the net rate of production of species I and the rate of creation by addition from the dispersed phase. Each species is denoted by the suffix *i*.

In this study, due to the non-reactive nature of the mixing of dyes, species transport was steered by mass diffusion caused by the diffusion flux, $\vec{J}$. This is dependent on the concentration and temperature gradient. Ficks Law, i.e. the dilute approximation method was used to describe the scalar transport.

Diffusion flux:

$$\vec{J}_i = -\rho D_{i,m} \nabla Y_i - D_{T,i} \frac{\nabla T}{T} \tag{2}$$

where $D_{i,m}$ is the mass diffusion coefficient for species I in the mixture and $D_{T,i}$ is the thermal diffusion coefficient.

C. Physical Geometry

Three MCFI geometries were constructed consisting of four straight coils connected with 90 degree bends in between, forming 4 arms of the MCFI. The inner tubing diameter (ID) was varied from 1.0mm, 0.8mm, and 0.5mm. The curvature ratio (λ) is the ratio of loop diameter over tubing diameter. The loop diameter (Dc) for each MCFI was modified to a curvature ratio of 10 corresponding to the tubing diameter.

In addition to MCFI, geometries of straight tube and straight coil with equivalent tube length used to construct the MCFI, as shown in Fig. 1, were also constructed to compare the mixing efficiency. Reynolds number of 250 was achieved in each individual MCFI through an adjustment of flow rate.

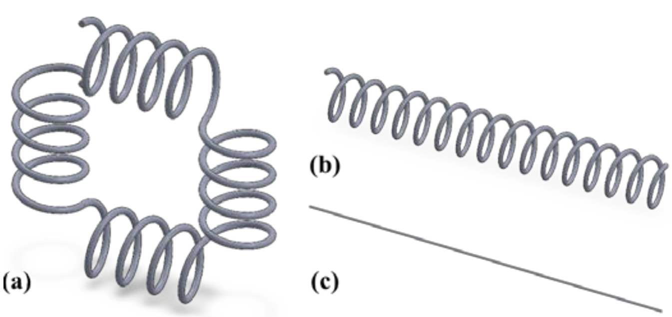

Fig. 1 Geometry design of (a) MCFI, (b) straight coil, and (c) straight tube with equivalent tube diameter and length

D. Mesh Topology

A non-uniform, unstructured grid topology was generated for computations of model equations. Three different mesh sizes constructed from hexahedral cells were generated, by varying the number of cross sectional and axial cells incrementally, as shown in Fig. 2. This led to three sets of mesh with total cells of 929556, 1474666 and 2457948. Grid independence was checked for the pressure drop within the MCFI. Pressure drop in units of Pascal was calculated to be 1732, 1743 and 1743 accordingly, which meant that the mesh size of 147466 was sufficient to shorten calculation time without compromising accuracy.

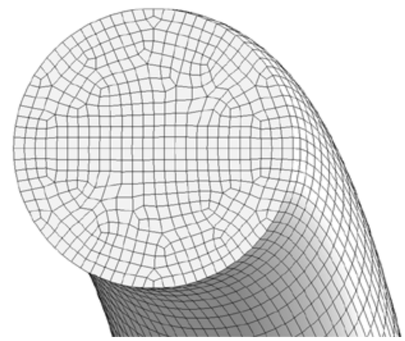

Fig. 2 Mesh topology at the inlet extended throughout the geometry

E. Mixing Efficiency

Simulation was initialized with half of the inlet as the entry for the red dye and half the inlet as the entry for the blue dye. Mixing of the fluids caused the mass fraction value of dyes change to signify mass transport.

Mixing is considered ideal when a cell contained equal parts of both fluid bodies, in this case, the water-based dyes, resulting in a local mass fraction of value of 0.5. An evaluation of the tube cross-section regarding the percentage of cells with a value of 0.5 represented the percentage of fluid mixing

$$Mixing\ Percentage, \theta = {N_{node=0.5}}/{N_{cross\ section\ nodes}} \times 100\% \tag{3}$$

III. RESULTS AND DISCUSSION

For validation, the velocity profile at different bends was generated with the proposed model and compared to the numerically computed results of published literature which focused on the process of heat transfer in MCFI. Fluid flow was simulated in MCFI ID of 0.5mm and λ of 10, similar to the geometry constructed for this study. Flow rate was adjusted to achieve Re of 434 as presented in literature.

Results of the horizontal and vertical centreline in Fig. 3 showed good agreement with the numerical prediction published in [6].

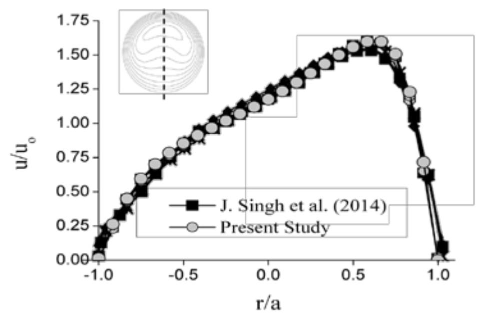

(a)

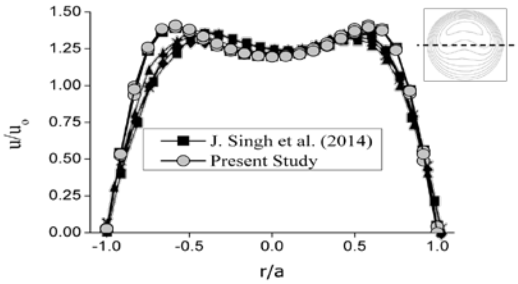

(b)

Fig. 3 Comparison of velocity profile in MCFI with data from literature for (a) verticle and (b) horizontal centerline

A. Velocity Profile

The velocity profile for fluid flow within the three different tubing configurations, which include straight tube, straight coil, and MCFI with tube diameter of 0.8 mm is shown in Fig. 4. For straight tube, the velocity profile was parabolic with a maximum velocity at the middle of the tube. This resembled a typical laminar flow profile.

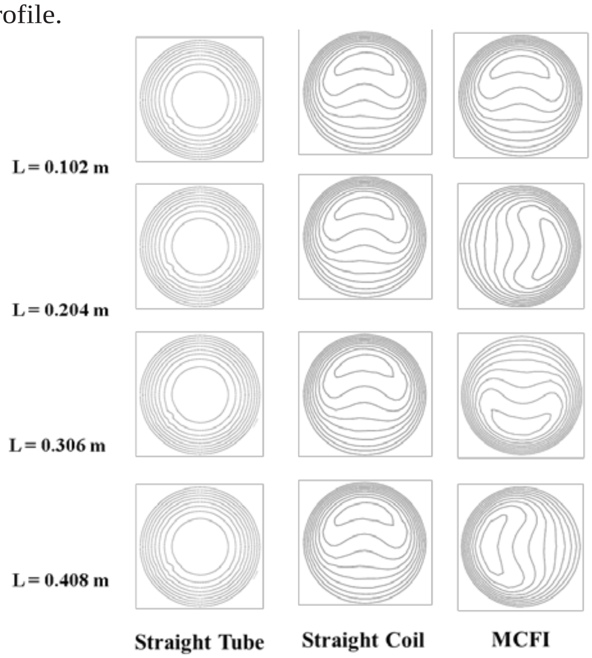

Fig. 4 Velocity profile in MCFI with ID 0.8 mm

For straight coil, the centrifugal force acting on fluid in the tubed caused the velocity profile to skew towards the outer wall, extended throughout the entire length of the tube.

Similar to the straight coil, the velocity profile for fluid flow in MCFI also skewed towards the outer wall. The presence of 90˚ bending between each arm caused the rotation of the velocity profile correspondingly, and the region of maximum velocity aligned in 4 different direction.

B. Mass Transport

Cross sectional visualisation of fluid flow within the MCFI in Fig. 5 showed a secondary flow exerted on the fluid. Mass fraction contour suggested such that high velocity fluid moved from the center of the tubing to the outer wall through the middle, while fluid at the outer wall moved along the upper and lower halves of the outer wall. As the region for maximum velocity was switched from side to side, the direction of secondary flow, in which fluid from high velocity region moved towards the outer wall, also rotated accordingly. This created a circular turbulence flow within the MCFI even in laminar flow condition. After the fluid passed the 90˚ bend, this phenomenon rotated accordingly.

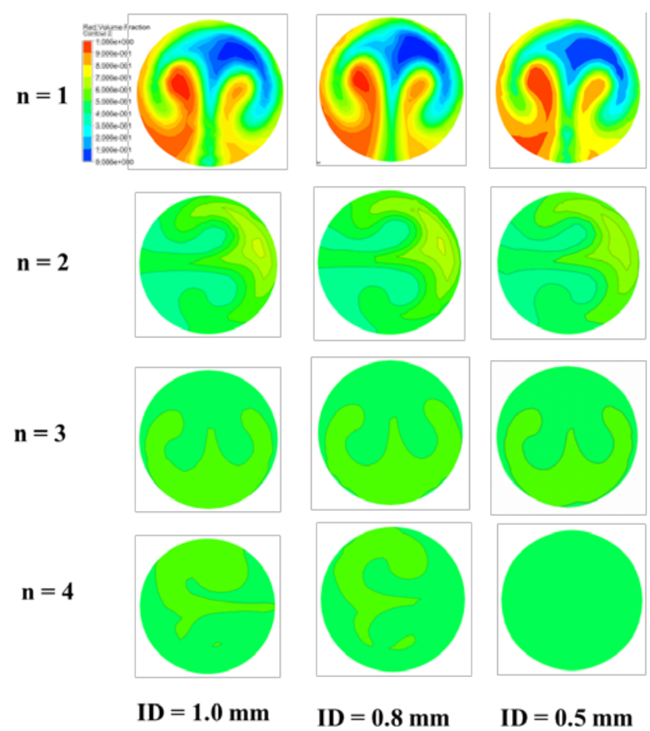

Fig. 5 Cross sectional mass fraction contour for MCFI

From the mass fraction contour, it can be seen that the fluid in all the MCFI with tube diameter 1.0 mm, 0.8mm and 0.5 mm had similar flow pattern and mixing profile. However, it was observed that complete mixing occurred in the fourth arm of the MCFI with ID 0.5 mm. Additional evaluation on the mixing profile of fluid in the MCFI was carried out by plotting the percentage of mixing over distance in travelled in tube length.

C. Mixing Plot

Fig. 6 shows the mixing plot for the MCFI, in which the percentage of mixing is plotted against tube length to indicate the distance travelled by the liquids before complete mixing occurs. MCFI mixing curves portrayed shoulders with increased rate of mixing, which corresponded to the 90˚ bends of MCFI, though the extent of increment in mixing rate varied. This observation supported that the presence of 90˚ bends improved the rate of mixing brought on by flow inversion.

MCFI with ID 1.0 mm showed the least rapid rate of mixing, and the liquids exited the MCFI with 54.5% mixing. MCFI with ID 0.8 mm showed slightly improved mixing rate, whereby the liquids exited the MCFI with 69.6% mixing.

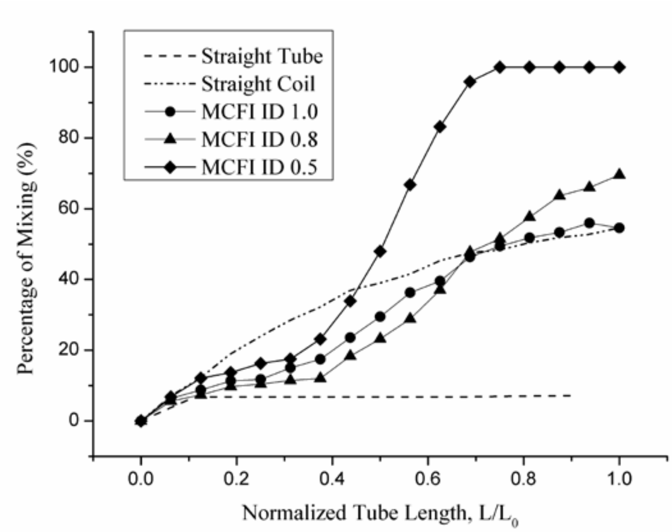

Fig. 6 Mixing plot for MCFI in comparison to straight tube and straight coil

Referring to the plotted graph, it can be perceived that only MCFI with the tubing diameter of 0.5 mm achieved complete mixing, at 0.69 normalized tube length equivalent to 175mm. MCFI with ID 0.5 mm did not show the gradual increment in mixing rate as presented with larger-sized tubing. Instead, the mixing rate resembled a sigmoidal curve, where it increased exponentially to achieve complete mixing.

Dyes in straight tube and straight coil were unable to achieve complete mixing with tube length equivalent to the construction of MCFI, even at smaller tubing diameter of 0.5 mm. Due to the high flow rate, the mixing rate in straight tube was almost flat-lined with 7% mixing, while straight coiled fared better with 54.6% mixing.

IV. CONCLUSION

Secondary flow was observed in the simulation of fluid flow in MCFI with tubing diameters 1.0mm, 0.8mm, and 0.5mm. Besides the variance in tubing diameter, other parameters such as pitch and curvature ratio of the MCFI were identical to avoid complexity during the evaluation of mixing. Water-based dyes in the MCFI displayed negligible differences in flow pattern and mass transfer process. Upon the analysis of mixing plot, the effect of tubing diameter was established. Complete mixing was only achieved in MCFI with tube diameter of 0.5mm before the fluid exited the MCFI. Larger tubing diameter led to incomplete mixing, even though the fluid flow has the same Re of 250. Though this finding might suggest that MCFI with smaller tubing diameter had more promising potential in mixing processes, further study can be carried out to verify this observation.

ACKNOWLEDGMENT

Both authors thank the support of Universiti Teknologi Malaysia in providing the facilities and software licensing for the implementation of this study.

REFERENCES

[1] V. Kumar, M. Aggarwal, and K. D. P. Nigam. "Mixing in curved tubes." *Chemical Engineering Science*. 2006; 61(17): 5742-5753.

[2] M. Mridha, and K.D Nigam. “Coiled flow inverter as an inline mixer.” *Chemical Engineering Science*. 2008 Mar; 63(6):1724-32.

[3] V. Kumar, M. Mridha, A.K. Gupta, and K. D. Nigam . “Coiled flow inverter as a heat exchanger.” *Chemical Engineering Science*. 2007 May; 62(9):2386-96.

[4] V. Kumar, and K.D. Nigam “Numerical simulation of steady flow fields in coiled flow inverter”. *International journal of heat and mass transfer*. 2005 Nov; 48(23):4811-28.

[5] M.M Mandal, P. Aggarwal, K.D. Nigam . “Liquid–liquid mixing in coiled flow inverter.” *Industrial & Engineering Chemistry Research*. 2011 Jul; 50(23):13230-5.

[6] J. Singh, N. Kockmann, K.D. Nigam . “Novel three-dimensional microfluidic device for process intensification.” *Chemical Engineering and Processing*: Process Intensification. 2014 Dec; 86:78-89.

[7] S.K. Kurt, M.G. Gelhausen, N. Kockmann. “Axial dispersion and heat transfer in a milli/microstructured coiled flow inverter for narrow residence time distribution at laminar flow.” *Chemical Engineering & Technology*. 2015 Jul; 38(7):1122-30.

[8] S.K. Kurt, I.V Gürsel, V. Hessel, K.D. Nigam, and N. Kockmann. “Liquid–liquid extraction system with microstructured coiled flow inverter and other capillary setups for single-stage extraction applications.” *Chemical Engineering Journal*. 2016 Jan 15; 284:764-77.

[9] L. Sharma, K. D. P. Nigam, and S. Roy. "Single phase mixing in coiled tubes and coiled flow inverters in different flow regimes." *Chemical Engineering Science*. 2017;160: 227-235.

[10] López-Guajardo, Enrique, et al. "Coiled flow inverter as a novel alternative for the intensification of a liquid-liquid reaction." *Chemical Engineering Science*. 2017, https://doi.org/10.1016/j.ces.2017.01.016.